The International Journal of Advanced Manufacturing Technology
https://doi.org/10.1007/s00170-024-14118-1

ORIGINAL ARTICLE

Implications of stress concentrators and work hardening in flat tensile samples subjected to milling and abrasive water jet machining

Luciano Buglioni[1] · Daniel Martínez Krahmer[1] · Antonio Sánchez Egea[2] · Alejandro Simoncelli[1,2,3]

Received: 19 June 2024 / Accepted: 8 July 2024

Abstract

The milling process is the standard method for producing flat tensile test specimens from sheet metal. However, alternative methods employed in the industry for cutting sheet metal include abrasive water jet cutting, laser cutting, punching, and, to a lesser extent, electrical discharge machining. Among these, abrasive water jet cutting stands out for its superior material integrity, versatility, precision, and efficiency, making it a preferred choice. Previous studies consistently show that specimens cut by abrasive water jetting exhibit lower ultimate tensile strength and higher percent elongation than those obtained by milling in standardized tensile tests. This study investigates this behavior across different types of steel and alloys. Both steel types were subjected to milling and water jetting processes, followed by an analysis of their experimental and simulated mechanical behavior to identify discrepancies between the two methods. The findings suggest that milling, influenced by factors such as feed per tooth and cutter diameter, introduces geometric stress concentrators. This relative increase in ultimate tensile strength and decrease in percent elongation are observed consistently in milled tensile specimens compared to those cut by water jet, regardless of material type or thickness. Additionally, the effects of perimeter hardening resulting from superficial plastic deformation caused by the cutting edge, likely due to its small thickness, do not influence the observed trends significantly.

Keywords Stress concentrator · Work hardening · Milling · Abrasive water jet · Tensile properties

1 Introduction

The mechanical properties of a sheet are typically characterized by constructing a specimen of standardized dimensions, with the axial axis parallel to the rolling direction, for tensile testing. International standards recognize milling as the only accepted manufacturing method for creating flat tensile specimens [1]. This method is preferred because milling is a well-established conventional process that allows for a wide range of cutting conditions and an almost unlimited variety of tools [2]. Other industrial methods for cutting sheet metal, such as laser cutting, abrasive water jet cutting (AWJC), and punching, are less suitable for producing flat tensile specimens. Laser cutting is generally avoided due to the heat-affected zone it creates, which alters the ductility of the cut perimeter [3]. Punching with a cutting die or a CNC punching machine induces significant hardening in the specimen's perimeter due to plastic deformation, rendering it unsuitable unless the hardened area is removed [4]. In contrast, AWJC is a common alternative due to its versatility and efficiency, allowing for producing specimens with mechanical properties representative of the sheet under study [5]. Despite this, all these processes—milling, laser cutting, AWJC, and punching—influence surface integrity [6], generating stress concentrators [7, 8] and microstructural modifications that can affect the ductility of the cut perimeter [9].

Milling significantly impacts the machined perimeter, as demonstrated by various studies. Santos et al. [10] found that strain hardening is influenced by the percentage of austenite in the deformed layer when working with duplex stainless steel.

✉ Antonio Sánchez Egea
antonio.egea@upc.edu

[1] Centro de Investigación y Desarrollo en Mecánica, Instituto Nacional de Tecnología Industrial INTI, Avenida General Paz 5445, 1650 Miguelete, San Martín, Provincia de Buenos Aires, Argentina

[2] Universitat Politècnica de Catalunya, Av. de Víctor Balaguer, 1, Vilanova i la Geltrú, 08800 Barcelona, Spain

[3] Facultad de Ingeniería, Universidad Nacional de Lomas de Zamora, Lomas de Zamora, Provincia de Buenos Aires, Argentina

Published online: 12 July 2024

Similarly, Sun and Guo [11], while machining a titanium alloy, observed an increase in surface hardness between 68 and 80%, noting that higher cutting speeds resulted in lower hardness due to thermal softening. Further research by Wang and Yu [12] on titanium alloy TC21 revealed that different lubrication methods—dry milling, high-pressure air cooling, and minimum quantity lubrication (MQL)—affect microscopic topography, surface roughness, and microhardness, with MQL effectively suppressing plastic deformation and surface defects. Xu et al. [13] studied the GH4169 superalloy and found that surface roughness and the depth of the plastic deformation layer differ little between wet and dry milling. However, surface microhardness is slightly lower in dry milling. Marakini and colleagues [14] reported that in high-speed milling of magnesium alloy, the type of insert (PVD or uncoated) and cutting conditions could increase hardness by 33 to 60% to a depth of about 50 µm, attributing this to milling forces and thermal softening. Lastly, Laamouri et al. [15] compared up-milling and down-milling of X160CrMoV12 steel, concluding that down-milling induces poor surface integrity with severe defects and reduces the fatigue limit by about 21% compared to up-milling.

Several publications have explored the impact of the AWJC process on the cut perimeter. For example, Hlavacova et al. [16] investigated the thermal adaptability of different steel grades subjected to various heat treatments, including normalization annealing, soft annealing, quenching, and quenching followed by tempering. They experimented with carbon steel C45, micro-alloyed steel 37MnSi5, and low-alloy steel 30CrV9, concluding that the homogeneity of the steel microstructure was crucial for cutting quality. They found that greater differences in hardness among structural components in an inhomogeneous microstructure resulted in higher surface roughness values. Gembalova and her co-workers [17] studied the comminution effect of #80 abrasive particles during and after cutting different materials, ranging from an aluminum alloy to tool steel. They discovered that the particles were significantly reduced in size, ranging from 8 to 24 µm, and that post-cut particles were similar in shape and size to those retained on the cut walls. In two related studies, Bankowski et al. [18, 19] examined the thermal transfer to the cut material caused by abrasion and plastic deformation from the abrasive particles. They noted that the amount of heat transferred depends on the material thickness and the cutting velocity, with thicker materials and lower velocities resulting in greater heat transfer. Specifically, for a 4.5-mm-thick S235JR steel cut at a feed rate of 50 mm/min, they measured an average hardness increase of 46% at about 20 µm from the edge using a nanodurometer [19].

Consequently, when determining the mechanical properties of a material through a tensile test on a specimen cut from a sheet, if the standard cutting method is milling, using an alternative process can modify these properties due to alterations in the surface integrity of the cut perimeters. Martinez Krahmer et al. [5] compared tensile specimens manufactured by milling and four alternative methods (laser, abrasive water jet, CNC punching, and wire EDM) on two very different materials—very low carbon steel (%C < 0.06) in three different thicknesses and Inconel 718. They found the AWJC process is the best alternative to milling, as it produces the smallest difference in mechanical properties. However, a consistent trend observed in all cases analyzed was that specimens cut by AWJC always showed decreased ultimate tensile strength (UTS) and increased elongation (A%) compared to those obtained by milling. Additionally, Goshert et al. [20] and Chang and co-workers [21] found similar trends, although they did not explain the reasons. This work aims to clarify why, across all materials and thicknesses tested, AWJC specimens consistently show increased elongation and reduced ultimate stress compared to milled specimens. To investigate this behavior, a new series of tensile tests were performed on milled and AWJC specimens from two steel plates (including one high-strength steel). The combined effects of stress concentration and hardening of the cut perimeter were analyzed, along with simulated semi-circular stress-concentrating tensile tests similar to those produced by the milling process. Therefore, the novelty of this work lies in evaluating whether the AWJC process could serve as a standard method for manufacturing flat tensile test samples in the industry, given its simplicity, and its advantages of low thermal impact and reduced mechanical stress.

2 Materials and methods

A total of 48 specimens were machined and tested. These specimens resulted from using two processes on two grades of steel (SPC 270 and SPC 980) with 12 repetitions each. Table 1 shows the nominal chemical composition by weight of the analyzed sheets, while Table 2 presents the geometric variability of the specimens, grouped by type of steel and process. This includes the average width in the reduced section (A), the associated standard deviation (σ), and the average taper in the reduced section (C).

Table 1 Chemical composition (% by weight) of SPC 270 and 980 steels

Steel	%C	%Si	%Mn	%P	%S	%Al	Hardness HV10
SPC 270	0.02	0.02	0.22	0.01	0.01	0.05	124.7 ± 8.6
SPC 980	0.17	1.40	2.00	0.02	0.002	—	304.0 ± 7.0

Table 2 Geometric variability of milling and AWJC specimens

Steel	AWJC			Milling		
	A (mm)	σ (mm)	C (mm)	A (mm)	σ (mm)	C (mm)
SPC 270	25.12	0.02	0.03	24.95	0.05	0.02
SPC 980	25.19	0.02	0.07	24.94	0.06	0.02

Table 3 Cutting conditions for both processes

Cutting parameters	Milling	AWJC
Feed rate (mm/min)	150	700
Spindle speed (rpm)	1060	Not apply

Table 3 shows the cutting conditions used in the milling and AWJC processes. The parameters for milling correspond to a 6-mm-diameter high-speed steel cutter used in the final contouring pass of the reduced section of the tensile specimens, machining a low to medium carbon steel. The cutting tool was a four-cutter at a feed rate per tooth of 0.035 mm/v and a 20 m/min cutting speed [22]. The conditions for the AWJC process were set according to the manufacturer's software (Flow Mach 3, model 1313b) based on the thickness of the steel sheet being cut (range 0.6 to 1 mm), using a stand-off distance of 2.5 mm, an offset of 0.5 mm, and a mass flow rate of 400 g/min.

The water jet machine has a 60,000-psi intensifier pump. It uses an abrasive called garnet #80, with an average diameter for the abrasive particles of 0.163 ± 0.113 mm (similar to the size indicated in [23]). Table 4 presents the semiquantitative analysis of garnet, resulting from the average of 5 measurements, similar to those reported by Hashish [24].

To eliminate the potential influence of residual stresses, all specimens were subjected to a stress-relieving process at 650 °C for 2 min [25] in an Indef 1250 °C–5.6 kW furnace. Figure 1 shows the set of machines and parameters used in the two methods studied to manufacture the flat tensile specimens.

3 Results and discussion

The results of this study are presented in the following subsections: tensile tests, stress–strain diagrams, effects of stress concentration, and finite element simulation.

3.1 Tensile tests

Regarding the geometric variability of specimens produced by both processes (see Table 2), the following observations arise: (1) AWJC process shows less dimensional variability among specimens, but they exhibit higher taper, especially in SPC 980 steel. (2) The milling process produces specimens with greater dimensional variability, albeit with lower taper.

Two main properties are considered for analysis regarding the results from tensile tests: UTS and percentage of elongation (A%). Table 5 shows the comparative values from previous studies, while Table 6 exhibits the materials studied in the current work. The results show the difference between UTS and elongation using the two methods for preparing flat tensile specimens: AWJC and milling. Based on the values presented in these two tables, the average percentage difference in UTS between specimens cut by AWJC and milling across all materials and thicknesses is −2.5%. Conversely, the average difference in elongation is +3.3%.

3.2 Stress–strain diagrams

The relationship between UTS and elongation is explored through relative pair diagrams for two types of cold-rolled carbon steels: SPC 270 and SPC 980. Figure 2 exhibits a comparative analysis of the mechanical properties of specimens machined using AWJC and milling processes. Specifically, it shows variations in UTS and elongation between the two cutting methods across the two material compositions.

In SPC 270 steel, a distinct trend is observed where milled specimens consistently demonstrate an increase in UTS alongside a reduction in elongation compared to those cut by AWJC. This trend underscores the effectiveness of milling in enhancing the material's UTS while compromising elongation, a characteristic often desirable in applications requiring high strength and structural integrity. Conversely, the trend is less pronounced in SPC 980 steel, suggesting a nuanced response to machining methods. Nevertheless, when averaging across SPC 980 specimens, those cut by AWJC show a modest decrease of −1.4% in UTS compared to milled specimens, accompanied by an average increase of +3.4% in elongation.

Table 4 Semiquantitative values of garnet components (% by weight)

% O	% Fe	% Si	% Al	% Mn	% Mg	% Ca
42.5 ± 4.0	24.3 ± 1.8	15.8 ± 2.0	10.0 ± 1.4	1.2 ± 0.8	2.0 ± 0.7	1.1 ± 0.5

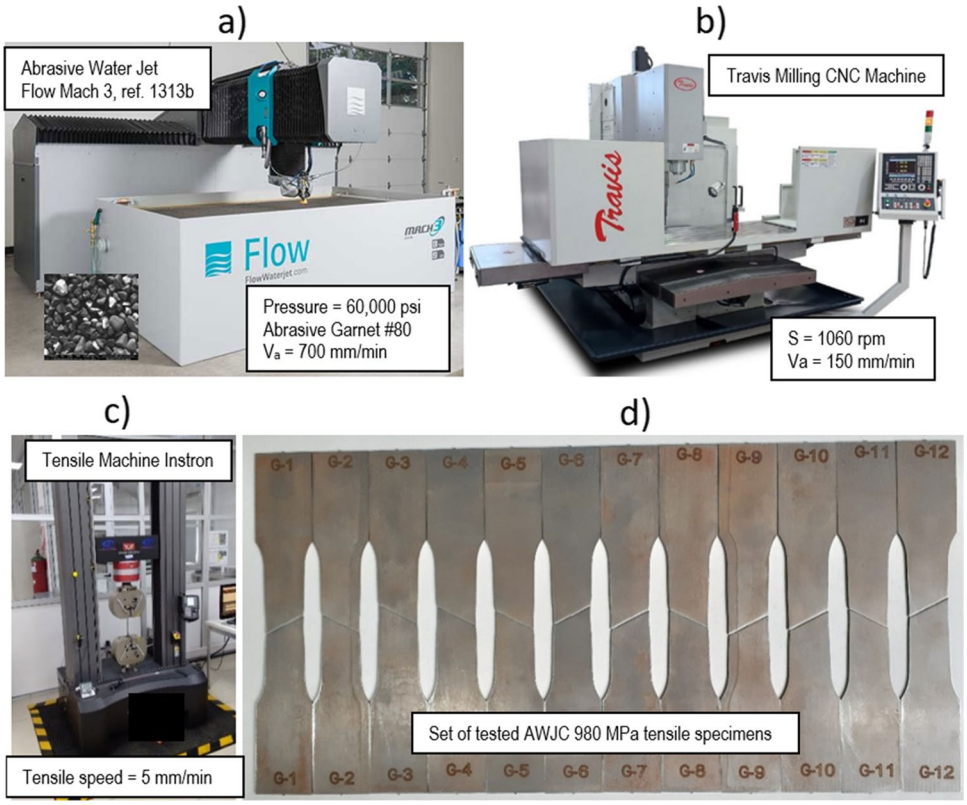

Fig. 1 Overall composition of the equipment and parameters used: **a** the AWJC machine and its cutting parameters; **b** the milling machine and its cutting parameters; **c** the universal tensile machine; **d** the steel tensile flat specimens

Table 5 Relative percentage differences for UTS and A% from previous studies [5]

Material	Thickness (mm)	Mechanical property	Difference %
Cold-rolled sheet of very low carbon steel (%C between 0.05 and 0.06)	0.5	UTS	−3.5
		A%	0.7
	1.0	UTS	−2.3
		A%	4.7
	1.5	UTS	−1.9
		A%	1.9
Inconel 718	5.0	UTS	−1.4
		A%	2.8

Table 6 Relative percentage differences for UTS and A% corresponding to the current study

Material	Thickness (mm)	Mechanical property	Difference %
Cold-rolled steel sheet SPC 270	0.6	UTS	−2.2
		A%	3.0
Cold-rolled high-strength steel sheet SPC 980	1.0	UTS	−1.4
		A%	3.4

This indicates that, on average, AWJC maintains a comparable trend in mechanical properties across both steels despite variations observed within SPC 980.

3.3 Effects of stress concentration

The systematic behavior observed in the mechanical properties of milled specimens versus those cut by AWJC is attributed to the interaction of the semi-circular stress concentration effect produced by the cutter diameter combined with the feed per tooth. To highlight the stress concentration effect, specimens were fabricated using AWJC from the material that exhibited greater sensitivity in distinguishing between cutting processes through mechanical properties (see Fig. 2), namely SPC 270 steel. Accordingly, a total of 16 specimens were machined and tested, comprising four types of sample notches (plain, line, triangle, and semi-circle) with four repetitions each. The radius at the bottom of the triangular notch is the minimum achievable value using the AWJC machine. Accordingly, Fig. 3 shows the notch geometries analyzed in the flat tensile specimens and the average values and percentage standard deviation among the different notches analyzed in SPC 270 carbon steel. The relative UTS is calculated with respect to the sample without a notch, which is assumed as the baseline.

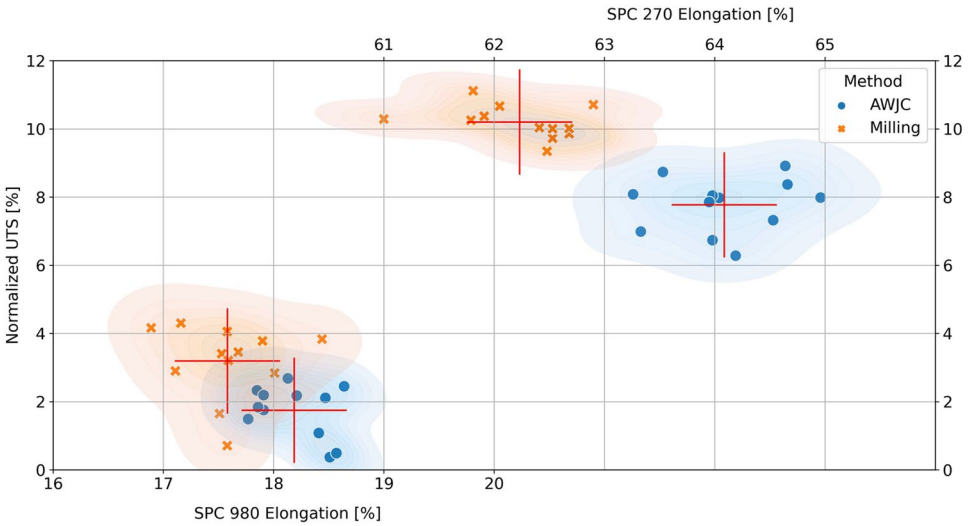

Fig. 2 Normalized UTS versus elongation for SPC 270 and SPC 980 carbon steels

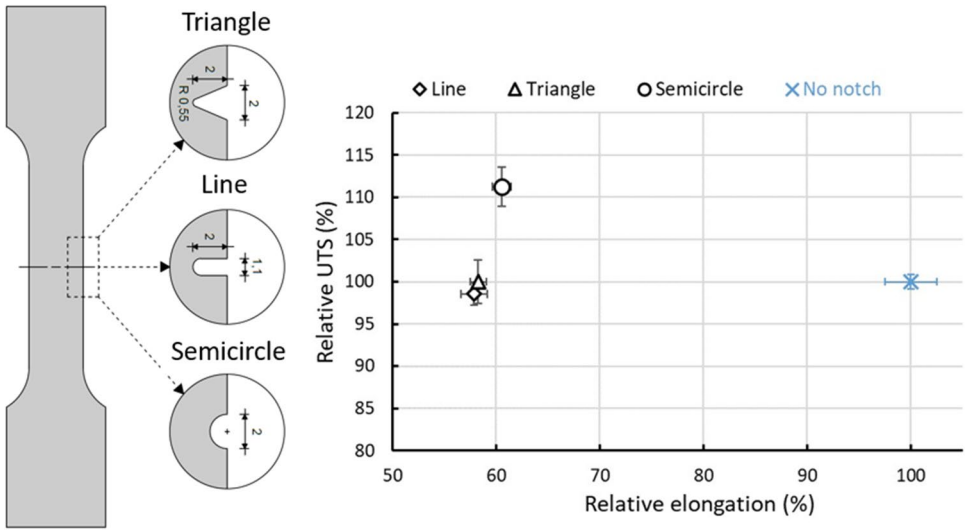

Fig. 3 Relative diagram UTS versus elongation for different SPC 270 carbon steel notch types. Note that the notch dimensions are in millimeters

Overall, the presence of notches does not substantially alter the UTS; however, it significantly reduces the percent elongation due to localized stress concentration. Similar results were reported by Goanta et al. [26]. In the specific case of specimens with a semi-circular notch, particularly concerning UTS, a more detailed analysis was conducted using finite element simulation to understand why UTS increases compared to notch-free specimens. It is observed that all notch shapes markedly decrease elongation, but those with a circular shape also increase UTS above 10%. This behavior resembles milled specimens, where a circular stress concentrator forms at the perimeter due to the combination of the cutter radius and the feed per tooth. According to Campbell [27], the stress concentration factor in specimens with semi-circular notches depends on the ratio between the notch radius and the width of the specimen. When using standardized specimens, only the notch radius remains as the variable factor.

Regarding the specimens of SPC 270 and SPC 980 steels, a summary of the absolute results obtained for UTS and A%, including the strain hardening coefficient SH, this coefficient can be obtained from a stress–strain diagram as indicated by Xu et al. [28]. Table 7 presents the disaggregated behavior of the coefficient by material and cutting process.

Upon analyzing Table 7, it becomes evident that tensile specimens cut by milling and AWJC from identical sheets exhibit distinct mechanical properties. Specifically, milled specimens consistently demonstrate lower elongation and higher UTS than those cut by AWJC. For SPC 270 steel, milling reduces elongation by an average of 3.0%, whereas for SPC 980 steel, the reduction is more pronounced at 3.4%. Conversely, UTS shows an average increase of 2.2% for SPC

Table 7 Results of UTS, A%, and SH in SPC 270 and SPC 980 carbon steels

Steel	Milling			AWJC		
	UTS (MPa)	A%	SH	UTS (MPa)	A%	SH
SPC 270	297.5	62.2	0.669	291.0	64.1	0.650
SPC 980	1011.3	17.6	0.322	997.1	18.2	0.316

270 and 1.4% for SPC 980 steel in the milled specimens compared to those cut by AWJC. Regarding strain hardening coefficient (SH), milling results in a 2.9% increase for SPC 270 steel specimens and a slightly lower increase of 1.9% for SPC 980 steel specimens compared to AWJC-cut specimens. This suggests that higher material strength correlates with a smaller change in strain hardening, thus narrowing the differences observed. This conclusion aligns with findings from other studies. For instance, Paetzold et al. [9] observed a significant increase in hardness in punch-formed specimens from high-strength DP800 steel. Meanwhile, Hilditch and Hodgson [29], in the case of punching an AA6111 aluminum alloy (low strength), using clearance between 5 and 51% of the thickness, achieved hardness increases of HV not less than 57% up to a maximum of 100%. Lastly, Dieter [30] states that if hardening increases, more stress is required to break the specimen.

The primary limitation of this study lies in the restricted scope of investigations into how cutting conditions affect geometric stress concentrators. In the AWJC process, conditions depend solely on the material type and thickness, leaving no other variables to experiment with. In contrast, milling allows for a wide variation in the diameter of the cutting tool, sharpness, material, and coating, potentially influencing the observed repetitive trends. Feed rates, in particular, significantly impact the effectiveness of cutting processes and the formation of geometric stress concentrators. Overall, lower feed rates are generally favorable for maintaining material integrity and controlling stress concentrators, whereas higher feed rates, although more efficient, pose risks to cut quality and structural soundness [31].

3.4 Finite element simulation

FEM models have been developed with ANSYS®. Simulation is quasi-static, considering the slow load speed. The elements used are 8-node (linear) hexahedra, and their formulation accounts for large displacements. Four different mesh configurations were analyzed for the smallest notch radius of 0.5 mm, ranging from 5000 to 20,000 elements. These configurations varied in mesh size and thickness. Results do not change significantly between meshes. Thus, a mesh of about 10,000 elements with a larger density at a notch location has been adopted for the final analysis. One-eighth of the probe is modeled for all cases, and displacements on the axial direction have been imposed.

Two types of finite element simulations were conducted on standardized tensile specimens, all 0.6 mm thick: (a) one considering the semicircular stress concentrator produced by the milling cutter diameter, and (b) another accounting for hardening around the specimen perimeter due to plastic deformation caused by the cutting edge. Given the heightened sensitivity in behavior (see Fig. 2), this section focused on SPC 270 steel. The mechanical behavior was reproduced by fitting an experimental Ludwik model to the material's obtained values, resulting in the specific equation $\sigma = 175 + 460\varepsilon^{0,65}$. Assuming a standardized cross-Sect. (25×0.6 mm) in all cases, semicircular stress concentrators with radii of 0.5, 2, and 3 mm were considered. Results indicated an increase in UTS and a decrease in A% with increasing radius, as depicted in Fig. 4. A radius of 3 mm was chosen since the contouring operation was performed with a 6-mm-diameter milling cutter.

This situation was simulated given the existing experimental evidence of how milling processes create a hardened subsurface zone beneath the machined surface. Initially, two specimens without notches were considered: one with a 20% [32] hardened perimeter and 100 µm thickness [33, 34] and another without hardening. In this first case, no modification was observed in the mechanical behavior curve of the analyzed specimens. Subsequently, the process was repeated with tensile specimens featuring 2-mm-radius semicircular notches (see Fig. 3), one with a 20% hardened perimeter and 100 µm thickness, and another without hardened perimeter. The same results were obtained in the previous case, indicating that the perimeter hardening did not affect the mechanical behavior. From the simulations conducted, it is concluded that the perimeter hardening caused by the cutting process does not appear to influence the achieved results. On the contrary, the semicircular stress concentrator characteristic of peripheral milling contributes to the increase in UTS and reduction in elongation of milled specimens compared to those cut by abrasive water jet machining. Supporting this observation, a study comparing punched tensile specimens with milled specimens obtained from the same sheets, ranging in thickness from 0.5 to 2.5 mm, showed that the punched perimeter exhibited a maximum average perimeter hardness increase of 64% compared to the original material with a plastic deformation affected depth of 0.65 mm. Despite such alteration, the UTS showed no significant changes [5].

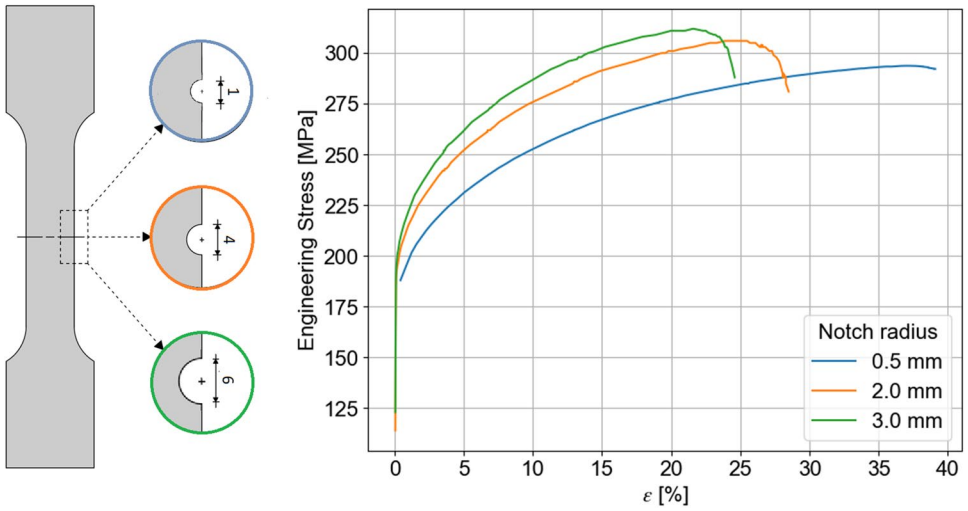

Fig. 4 Reproduction of the mechanical behavior of SPC 270 steel with different notch radii. Note that the notch dimensions are in millimeters

To further enhance the accuracy and efficiency of the FEM analysis, it would be advantageous to incorporate automatic remeshing during the deformation process. This approach offers significant benefits, including reducing computational time and the precise representation of large strains, particularly at critical points such as notches. The dynamic adjustment of the mesh ensures that the model maintains high resolution in areas experiencing substantial deformation, thereby improving the fidelity of the stress–strain curve analysis. Preliminary tests using the MOOSE (Multiphysics Object Oriented Simulation Environment) open-source software have already demonstrated the potential of this method. These initial experiments indicate that MOOSE's capabilities in adaptive meshing and handling complex multiphysics problems are promising for our specific application. In addition to refining the mesh adaptation strategy, exploring the effects of different notch geometries is crucial. Variations in notch shape can significantly influence the local stress distribution and strain concentration, impacting the overall mechanical behavior of the material. By systematically analyzing different notch configurations, we can better understand the stress–strain response and identify any critical geometrical features that may exacerbate or mitigate material failure. Future studies should include a detailed comparison between the stress–strain curves obtained from models with automatic remeshing and those from traditional static mesh approaches. Moreover, the influence of various notch shapes on mechanical performance should be thoroughly investigated, potentially leading to optimized designs that enhance durability and resistance to failure under load.

4 Conclusions

The main conclusions derived from this study can be summarized as follows:

- The feed per tooth in milling generates a semicircular geometric stress concentrator on the cut surface, with its magnitude scaling with the radius of the milling cutter employed. This geometric feature significantly influences mechanical properties in specimens cut by milling compared to AWJC, resulting in an average increase in UTS of + 2.2% for SPC 270 steel and + 1.4% for SPC 980 steel, along with a decrease in elongation by − 3.0% for SPC 270 steel and − 3.4% for SPC 980 steel.
- The mechanical properties of notched specimens by milling exhibit a predictable decrease compared to unnotched specimens. Circular notches demonstrated about 10% superior UTS among the various notch geometries tested due to their less severe stress concentration effects. Additionally, AWJC also creates a geometric stress concentrator, but due to the significantly reduced particle size post-cutting (8 to 24 µm), its impact on mechanical properties resembles that of a zero-radius notch.
- Simulations revealed that specimens with a 20% hardened perimeter and 100 µm thickness showed no significant deviation in mechanical behavior compared to those without hardening. Furthermore, specimens featuring 2-mm semicircular notches confirmed that perimeter hardening did not alter mechanical properties noticeably.

Acknowledgements The authors thank Martín Gadaleta from MARO company for providing the sheet metals used in this study and machining the milled specimens. Additionally, thanks are extended to María Paula Martinez for creating some of the figures included in this work and to Professor Lucio Iurman for his careful review of the manuscript and valuable comments received.

Author contribution All authors contributed to the study's conception and design. Luciano and Alejandro performed material preparation, data collection, and analysis. Daniel wrote the first draft of the manuscript. Antonio worked on editing and formatting the manuscript. All

authors commented on previous versions and read and approved the final manuscript.

Funding Open Access funding provided thanks to the CRUE-CSIC agreement with Springer Nature. This research work was supported by the Serra Húnter program (Generalitat de Catalunya).

Declarations

Ethics approval There are no ethical conflicts.

Consent to participate The study did not include humans or animals.

Consent for publication Included in submission.

Competing interests The authors declare no competing interests.

References

1. ASTM Standard E08M-04 (2004) standard test methods for tension testing of metallic materials. ASTM International. https://doi.org/10.1520/E0008M-04
2. Matuszak J, Zaleski K, Zysko A (2023) Investigation of the impact of high-speed machining in the milling process of titanium alloy on tool wear, surface layer properties, and fatigue life of the machined object. Materials 16:5361. https://doi.org/10.3390/ma16155361
3. Son S, Lee D (2020) The effect of laser parameters on cutting metallic materials. Materials 13:4596. https://doi.org/10.3390/ma13204596
4. Paetzold I, Dittmann F, Feistle M, Golle R, Haefele P, Hoffmann H, Volk W (2017) Influence of shear cutting parameters on the fatigue behavior of a dual-phase steel. J Phys: Conf Ser 896:012107. https://doi.org/10.1088/1742-6596/896/1/012107
5. Martinez Krahmer D, Polvorosa R, López de Lacalle LN, Alonso-Pinillos U, Abate G, Riu F (2016) Alternatives for specimen manufacturing in tensile testing of steel plates. Exp Tech 40:1555–1565. https://doi.org/10.1007/s40799-016-0134-5
6. Suárez A, Veiga F, Polvorosa R, Artaza T, Holmberg J, López de Lacalle LN, Wretland A (2019) Surface integrity and fatigue of non-conventional machined alloy 718. J Manuf Process 48:44–50. https://doi.org/10.1016/j.jmapro.2019.09.041
7. Liu G, Huang C, Zhao B, Wang W, Sun S (2021) Effect of machined surface integrity on fatigue performance of metal workpiece: a review. Chin J Mech Eng 34:1–16. https://doi.org/10.1186/s10033-021-00631-x
8. Arola D, Williams C (2002) Estimating the fatigue stress concentration factor of machined surfaces. Int J Fatigue 24(9):923–930. https://doi.org/10.1016/s0142-1123(02)00012-9
9. Paetzold I, Feistle M, Golle R, Volk W, Frehn A, Ilskens R (2018) Determination of the minimum possible damage due to shear cutting using a multi-stage shear cutting process. Mater Sci Eng 418:012070. https://doi.org/10.1088/1757-899X/418/1/012070
10. Santos C, Carneiro J, Cordeiro G, Brito P, Santos I, Campos T (2021) Residual stress and surface microhardness post-milling in 2205 duplex steel. Int J Adv Manuf Technol 113:1–11. https://doi.org/10.1007/s00170-021-06829-6
11. Sun J, Guo Y (2009) A comprehensive experimental study on surface integrity by end milling Ti–6Al–4V. J Mater Process Technol 209:4036–4042. https://doi.org/10.1016/j.jmatprotec.2008.09.022
12. Wang Z, Li H, Yu T (2022) Study on surface integrity and surface roughness model of titanium alloy TC21 milling considering tool vibration. Appl Sci 12:4041. https://doi.org/10.3390/app12084041
13. Xu R, Zhou Y, Li X, Yang S, Han K, Wang S (2019) The effect of milling cooling conditions on the surface integrity and fatigue behavior of the GH4169 superalloy. Metals 9:1179. https://doi.org/10.3390/met9111179
14. Vi M, Pai P, Bhat B, Thakur D, Achar B (2022) High-speed face milling of AZ91 Mg alloy: surface integrity investigations. Int J Light Mater Manuf 5:528–542. https://doi.org/10.1016/j.ijlmm.2022.06.006
15. Laamouri A, Ghanem F, Braham C, Sidhom H (2019) Influences of up-milling and down-milling on surface integrity and fatigue strength of X160CrMoV12 steel. Int J Adv Manuf Technol 105:1209–1228. https://doi.org/10.1007/s00170-019-04280-2
16. Hlavacova I, Sadílek M, Vanova P, Szumilo S, Tyc M (2020) Influence of steel structure on machinability by abrasive water jet. Materials 13(19):4424. https://doi.org/10.3390/ma13194424
17. Gembalová L, Hlavac L, Spadlo S, Geryk V, Oros L (2021) Notes on the abrasive water jet (AWJ) machining. Materials 14:7032. https://doi.org/10.3390/ma14227032
18. Spadlo S, Bankowski D, Mlynarczyk P, Hlavacova I (2021) Influence of local temperature changes on the material microstructure in abrasive water jet machining (AWJM). Materials 14:5399. https://doi.org/10.3390/ma14185399
19. Bankowski D, Mlynarczyk P, Hlavacova I (2022) Temperature measurement during abrasive water jet machining (AWJM). Materials 15:7082. https://doi.org/10.3390/ma15207082
20. Goshert B, Terrazas O, Matlock D, Van Tyne C (2018) Sample edge effects on tensile properties and sheet formability. IOP Conf Ser: Mater Sci Eng 418:012064. https://doi.org/10.1088/1757-899x/418/1/012064
21. Chang Y, Zhang J, Han S, Li X, Yu S (2023) Influence of cutting process on the flanging formability of the cut edge for DP980 steel. Metals 13:948. https://doi.org/10.3390/met13050948
22. Machining data handbook (1997), Vol 1, 3th Edition, Cincinatti, USA, ISBN-13 978-0936974002
23. Perec A, Radomska-Zalas A, Fajdek-Bieda A, Kawecka E (2022) Efficiency of tool steel cutting by water jet with recycled abrasive materials. Materials 15:3978. https://doi.org/10.3390/ma15113978
24. Hashish M (2010) AWJ milling of gamma titanium aluminide. J Manuf Sci Eng 132(4):041005. https://doi.org/10.1115/1.4001663
25. Nivas R, Das G, Das S, Mahato B, Kumar S, Sivaprasad K, Ghosh M (2016) Effect of stress relief annealing on microstructure & mechanical properties of welded joints between low alloy carbon steel and stainless steel. Metall Mater Trans A 48(1):230–245. https://doi.org/10.1007/s11661-016-3840-9
26. Goanta V, Mares M, Axinte T (2016) The stress raisers effects on the materials mechanical characteristics, analyzed by local microhardness measurements. IOP Conf Ser: Mater Sci Eng 147:012102. https://doi.org/10.1088/1757-899x/147/1/012102
27. Campbell F (2012) Fatigue and fracture: understanding the basics. ASM International, ISBN: 978–1–61503–976–0

28. Xu L, Schultheiss F, Andersson M, Ståhl J (2013) General conception of polar diagrams for the evaluation of the potential machinability of workpiece materials. Int J Mach Mach Mater 14(1):24–44. https://doi.org/10.1504/ijmmm.2013.055119
29. Hilditch T, Hodgson P (2005) Development of the sheared edge in the trimming of steel and light metal sheet. J Mater Process Technol 169(2):192–198. https://doi.org/10.1016/j.jmatprotec.2005.02
30. Dieter GE (1988) Mechanical metallurgy. McGraw-Hill Book Company, London
31. Ezugwu EO (2005) Key improvements in the machining of difficult-to-cut aerospace superalloys. Int J Mach Tools Manuf 45(12–13):1353–1367
32. Yang D, Liu Z (2018) Surface integrity generated with peripheral milling and the effect on low-cycle fatigue performance of aeronautic titanium alloy Ti-6Al-4V. Aeronaut J 122(1248):316–332. https://doi.org/10.1017/aer.2017.136
33. Arif R, Fromentin G, Rossi F, Marcon B (2020) Investigations on strain hardening during cutting of heat-resistant austenitic stainless steel. J Manuf Sci Eng 142(5):051005. https://doi.org/10.1115/1.4046612
34. Xu D, Ding L, Liu Y, Zhou J, Liao Z (2021) Investigation of the influence of tool rake angles on machining of Inconel 718. J Manuf Mater Process 5:100. https://doi.org/10.3390/jmmp5030100